


 Cite this: *Chem. Commun.*, 2025, 61, 5585

 Received 31st January 2025,
 Accepted 12th March 2025

DOI: 10.1039/d5cc00577a

rsc.li/chemcomm

A photo-switchable surfactant possessing a spiropyran-moiety in its backbone – unravelling the structure of micelles with small-angle neutron scattering (SANS) and transmission electron microscopy (TEM)†

 Marek Bekir,^a Matthias Schenderlein,^b Jakob Ruickoldt,^c Petra Wendler,^c Joachim Kohlbrecher,^d Ingo Hoffmann^{b,e} and Martin Reifarth^{b,f}

We use SANS and TEM to elucidate the shape of the micelles that a spiropyran (SP) surfactant forms. Being both pH- and photo-switchable to a less surface active merocyanine (MC) form, we find that their micelles are of cylindrical shape in any case, which leads us to conclude that the surfactant always switches to its SP form when micellising.

The capability to alter their surface-active behaviour upon the activation with light (and potentially other stimuli) renders photo-responsive surfactants useful auxiliaries for the manipulation of colloidal systems.¹ Literature provides various examples, where the switching state-dependent tendency to assemble at an interface is exploited in different applications. Accordingly, switchable surfactants are used to control active motion of microscale particles,^{2–4} the stability of emulsions^{5,6} or foams,^{7,8} the morphology of a polyelectrolytes,⁹ or they are used to manipulate the shape of a polymeric nanoparticle consisting of different blocks^{10,11} among many other examples.

On a microscopic level, light irradiation alters the shape and size of the micelles formed by photo-switchable surfactants.^{12,13} As an example, azobenzene compounds have been shown to exhibit assembly geometries that are significantly affected by switching, which in turn affects the viscosity of the medium.^{14,15} More complex surfactant architectures provide even more notable

changes in the assembly architecture, such as transitioning from spherical to worm-like micelles to lamellar bilayers^{16,17} or they may be used to fabricate switchable vesicles.¹⁸ Along with the high significance of azobenzene surfactants, as it is reflected in the large number of reports on this topic,¹ these systems have been investigated actively regarding their structural details. Alternative systems, that are, *e.g.* based on azopyrazole, are not so prominent, so that there are only few studies focussing on investigations of their switching behaviour.^{19,20} In recent years, surfactants based on other photo-switchable systems,²¹ such as spiropyrans, gained increasing interest.^{11,22–26} Spiropyran is a photosystem that undergoes a ring-opening reaction from an electrically neutral to a zwitterionic betain molecule.²⁷ Recently, we reported a novel system, which constitutes a surfactant, in which the spiropyran unit is introduced into its hydrophobic backbone.⁶ It has been shown, that this system alters its surface-activity (as characterized by the critical micelle concentration, CMC) under acidic conditions, which, in contrast, remains unaffected at a neutral and alkaline pH value. In our previous work,⁶ we proposed a plausible explanation of this observation, based on spectrochemical evidence and quantum-chemical calculations.

The present study aims to underline the hypothesized switching and micellization behaviour with experimental methods suitable for this purpose, *i.e.* SANS and TEM. It is therefore crucial to understand the stability of the different switching states in an aqueous environment (Fig. 1).

In an aqueous environment, spiropyran molecules can be present in the zwitterionic merocyanine (MC) or the non-ionic spiropyran (SP) form (Fig. 1).⁶ Being obtained as SP derivative, the surfactant readily dissolves in water to form a deep-red solution (Fig. 1). The red colour is indicative for the formation of the MC form, being the thermodynamically stable form in an aqueous environment due to its zwitterionic nature.²⁷ In MilliQ water, thus, we observe an equilibrium of the MC and the SP form, which is significantly shifted to the MC form. Illumination with blue light (455 nm) will foster the switching to the SP form.

^a Institute of Physics and Astronomy, University of Potsdam, Karl-Liebknecht-Str. 24-25, D-14476 Potsdam, Germany. E-mail: marek.bekir@uni-potsdam.de

^b Fraunhofer Institute of Applied Polymer Research, Geiselbergstr. 69, D-14476 Potsdam, Germany

^c Institute of Biochemistry and Biology, University of Potsdam, Karl-Liebknecht-Str. 24-25, D-14476 Potsdam, Germany

^d PSI Center for Neutron and Muon Science, Forschungsstr. 111, CH-5232 Villigen PSI, Switzerland

^e Institut Max von Laue-Paul Langevin (ILL), 71 Avenue des Martyrs, CS 20156, F-38042 Grenoble Cedex 9, France. E-mail: hoffmann@ill.fr

^f Institute of Chemistry, University of Potsdam, Karl-Liebknecht-Str. 24-25, D-14476 Potsdam, Germany. E-mail: martin.reifarth@uni-potsdam.de

† Electronic supplementary information (ESI) available. See DOI: <https://doi.org/10.1039/d5cc00577a>



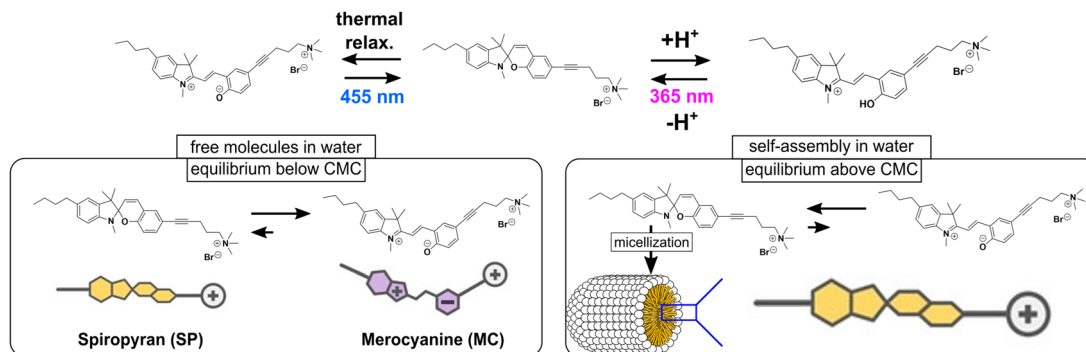


Fig. 1 Schematic representation of the photophysical behaviour of the surfactant as well as its behaviour in MilliQ water.

At a concentration ≥ 0.7 mM, the illuminated surfactant in its SP form will micellise, corresponding to the CMC of the SP surfactant (Fig. 2).⁶ Interestingly, a similar CMC of 1.0 mM is determined, when the solution is not illuminated and, thus, the MC form of the molecule is predominant in solution $<$ CMC (Fig. 2).⁶ Given the structure of the molecule in its MC form (Fig. 1, left) possessing a zwitterionic moiety in its hydrophobic chain, it seems somewhat surprising at a first glance, that the molecule forms micelles at almost the same concentration as the molecule in SP form that does not possess any charged groups along its hydrophobic part. We explain this behaviour by the spontaneous formation of SP, after which the SP molecules will assemble to form the micelles.⁶ Under acidification, the MC is protonated to form MCH^+ (Fig. 1). This species can be switched to the SP form upon illumination with blue light.

In this form, the CMC of this surfactant could be determined as 0.7 mM, which corresponds to the CMC of the SP in the neutral form (Fig. 2). Accordingly, we hypothesize that all the merocyanine species first switch to the SP form, in which they assemble to micelles.

For structural elucidation, we use SANS to investigate micelle morphology with high statistical validity,²⁸ effectively resolving surfactant micelles' typical sizes in the low nanometre range.²⁹ The SANS scattering curves are displayed in Fig. 3. For all investigated samples, the chosen concentration of 10 mM is

significantly above the CMC, while it would still be below the CMC under acidic pH conditions in the dark.

The scattering curves from 10 mM surfactant solution at neutral pH in the dark and under irradiation with blue light look nearly identical (Fig. 3a). All curves show a q^{-1} slope in the mid q range

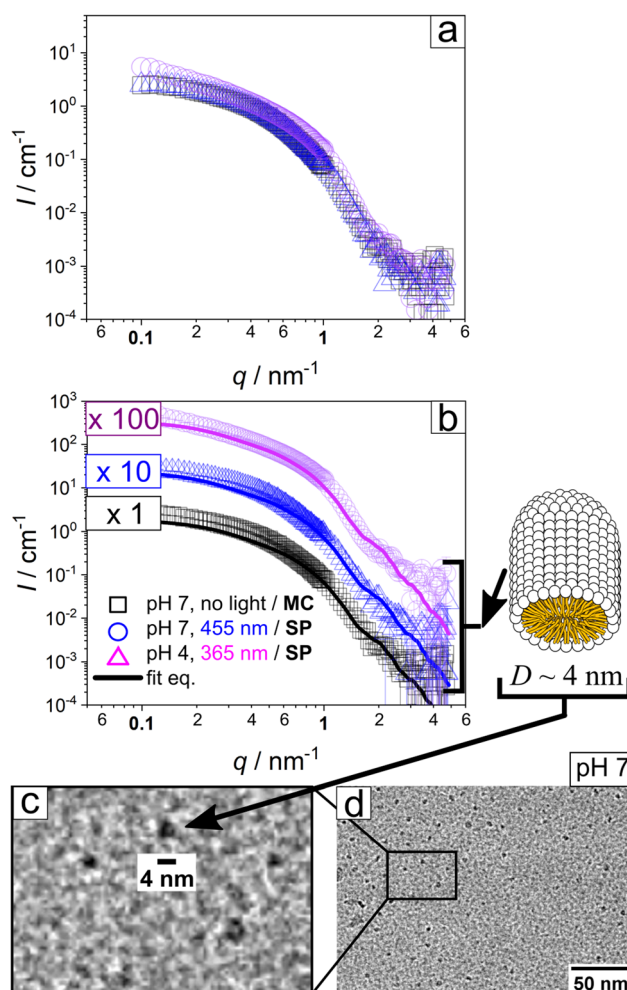


Fig. 3 Structural elucidation of the micelles. (a) SANS scattering curves of the micelles forming (including a schematic representation of the micelle) at (i) a neutral pH value in the dark, (ii) a neutral pH after irradiation with blue, (iii) an acidic pH value with blue irradiation. (b) Stacked scattering curves with model fit. (c) and (d) TEM micrographs.

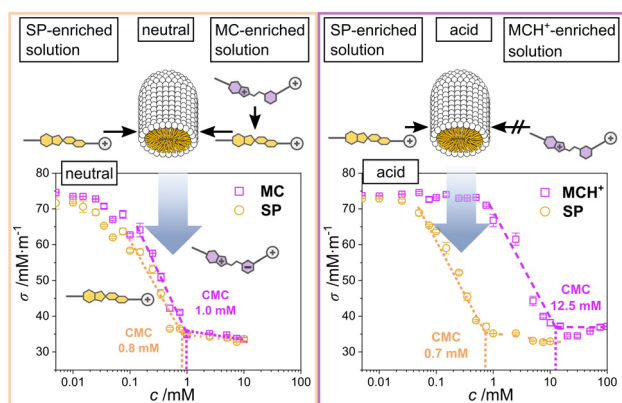


Fig. 2 CMC values of the surfactant at an acidic and a neutral/basic pH value. The data is reproduced from ref. 6.



from about 0.2 to 0.7 nm^{-1} which indicates that the micelles have an elongated structure (Fig. 3b, for clarity, the curves are stacked). The smeared-out form factor oscillation at 1.8 nm^{-1} shows that the micelles have the same small dimension under all conditions and the transition from a plateau to a q^{-1} slope at about 0.2 nm^{-1} shows that also the long dimension of the micelles is similar. The volume fraction ϕ obtained from invariant analysis $Q = \int q^2 I(q) dq = 2\pi(\Delta\text{SLD})^2 \phi(1 - \phi)$, where ΔSLD refers to the difference in scattering length density between solvent and micelles, is in good agreement with the expected value for a 10 mM sample. Further information of the fitting is provided in the ESI† of the article.

The determined radius of the micelle of about 1.8 nm is compatible with the length of the molecule in its SP form. Along with the fact, that the shape of the micelles seems to be identical under all conditions, it seems highly likely that the surfactant switches from the MC to the SP form whenever micellising. This observation is in contrast to azobenzene surfactants, where different micellar shapes were observed depending on the surfactant's switching state.³⁰

For comparison, we conducted cryogenic TEM (cryo-TEM) of the micelle solution of a neutral sample kept in the dark. Similar size regimes were determined, where micelles with diameters of approximately 4 nm (Fig. 3c) could be obtained. Additional micrographs revealing the micellar anisotropy more pronouncedly are provided in Fig. S1 (ESI†, note that TEM micrographs represent a projection of the sample).

At a low pH value, the surfactant is present in its MCH^+ form. Irradiation with blue light fosters the switching $\text{MCH}^+ \rightarrow \text{SP}$. The scattering curve of this case looks identical to the scattering curves of the SP form as previously described (Fig. 3a and b), indicating that in the three different cases, *i.e.* dark and illuminated at a neutral as well as illuminated at an acidic pH value, the same micelles occur.

Despite its permanent, dual-positive charge rendering the surfactant in its MCH^+ form well water-soluble under acidic and non-illuminated conditions, the surfactant will form micelles at a concentration $\geq 12.5 \text{ mM}$. Here, we again assume that the protonated merocyanine may spontaneously switch to the SP form ($\text{MCH}^+ \rightarrow \text{SP} + \text{H}^+$), which in turn will form the micelles. For elucidation, we conducted proton nuclear magnetic resonance (^1H NMR) spectroscopy. Fig. 4a shows the respective ^1H NMR spectra recorded in deuterated water (D_2O , peak assignment further explained in Fig. S2, ESI†). The spectrum clearly reveals a difference in the aromatic region between the two concentrations, pointing towards the predominant presence of the MCH^+ molecules at concentrations below and the SP form above the CMC. Having shown that the SP form is predominant $\geq \text{CMC}$, we conducted cryo-TEM for structural elucidation. In the corresponding micrographs, we see the formation of micelles with slightly heterogenous appearance (additional micrographs are provided in Fig. S1, ESI†). In the projection, a diameter of $\sim 4 \text{ nm}$ is observed. The size of the micelles is in good agreement with that obtained from the SP micelles. On the basis of this data, we deduce that the MCH^+ species first switch to the SP species, which assemble to the micelles.

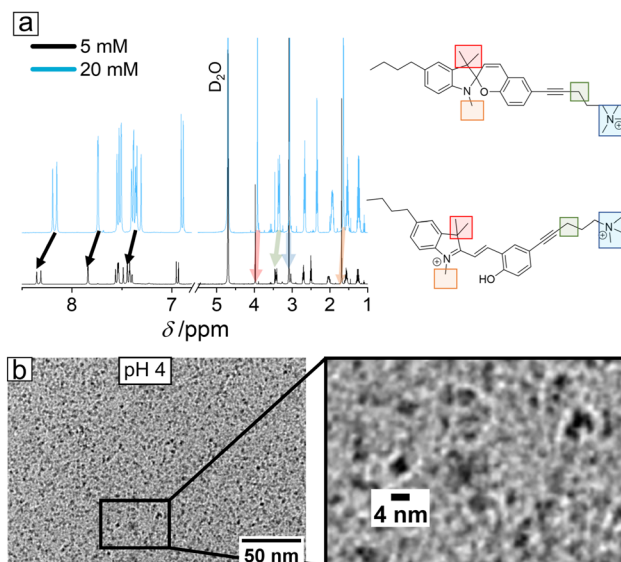


Fig. 4 MCH^+ micelles in the dark. (a) Comparison of ^1H NMR of the surfactant $> \text{CMC}$ and $< \text{CMC}$ in D_2O . (b) Cryo-TEM micrograph of the solution (20 mM) at an acidic pH value.

In order to understand the interaction with respect to thermodynamics, we conducted isothermal titration calorimetry measurements (ITC), where all species were kept in the dark.

Thus, we used a solution with the surfactant under acidic or neutral conditions both far above the CMC and titrated it in (1) MilliQ water or (2) acidic water ($\text{pH} \sim 4$).

We observe the reaction enthalpies ΔH of the de-micellization (and subsequent) processes, when we dilute the micelle-containing solution during titration (see Fig. S3, ESI†). (1) First we discuss the titration against MilliQ water, where we observe an endothermic reaction with a value of $\Delta H = (15 \pm 1) \text{ kJ mol}^{-1}$. The latter comprises two processes measured simultaneously: (i) de-micellization of the molecules being present in SP and (ii) the subsequent switching from the less stable SP into more stable MC-form in water.⁶

(2) When the reaction is conducted at a pH value of 4, we observe a less endothermic reaction with a value of $\Delta H = (8 \pm 4) \text{ kJ mol}^{-1}$. This reaction encompasses three elementary reactions by first a (i) de-micellization *via* dilution, (ii) then a switching from SP into more stable MC form in water, followed by (iii) a protonation $\text{MC} + \text{H}^+ \rightarrow \text{MCH}^+$ under acidic conditions. Enthalpy values point towards a less endothermic reaction compared to the dilution of the surfactant at a neutral pH level (see Fig. S3b, ESI†). In order to elucidate the $\text{MC} + \text{H}^+ \rightarrow \text{MCH}^+$ process, we titrated the surfactant at a concentration $< \text{CMC}$ by successively adding an aqueous solution of trifluoroacetic acid (TFA). The protonation reaction is a rather exothermic reaction (Fig. S3c, ESI†).

Accordingly, we explain the less endothermic reaction of the de-micellization of the surfactant under acidic conditions, compared to the more pronounced process under neutral conditions, by the fact that the exothermic protonation reaction to MCH^+ compensates the endothermic de-micellization. Note, that the ΔH values cannot be compared quantitatively, given



the fact that the measurements were conducted in solutions possessing different ionic strengths.

In conclusion, we demonstrate that spiropyran-based surfactants tend to self-assemble into the SP form, despite the MC form being the more stable form in water. This suggests that only one micellar type exists based on the micelles of the surfactant in the SP form. Only protonation inhibits the tendency to self-assemble and shifts the CMC towards higher concentration presumably due to the exothermic protonation reaction to MCH⁺, which compensates the endothermic demicellization.

M. B. and M. R. acknowledge financial support by the German Research Foundation (DFG) through the grant with the project numbers 469240574 (M. B.) and 471323994 (M. R.). The authors acknowledge Melanie Anding and Jeanette Wenzel for their support with cryo-TEM measurements. The authors thank the Paul Scherrer Institute (PSI) for Beam line time as well as the PSCM laboratory for facilitating density measurements.

Data availability

The data supporting this article have been included as part of the ESI.† The data shown in Fig. 2 are reproduced from ref. 6.

Conflicts of interest

There are no conflicts to declare.

Notes and references

- 1 S. Santer, *J. Phys. D: Appl. Phys.*, 2017, **51**, 013002.
- 2 P. Arya, M. Umlandt, J. Jelken, D. Feldmann, N. Lomadze, E. S. Asmolov, O. I. Vinogradova and S. Santer, *Eur. Phys. J. E: Soft Matter Biol. Phys.*, 2021, **44**, 50.
- 3 J. Vialto, M. Anyfantakis, S. Rudiuk, M. Morel and D. Baigl, *Angew. Chem., Int. Ed.*, 2019, **58**, 9145–9149.
- 4 M. Bekir, A. Sharma, M. Umlandt, N. Lomadze and S. Santer, *Adv. Mater. Interfaces*, 2022, **9**, 2102395.
- 5 S. Biswas, S. Karishma, B. Ramesh, M. Jeganmohan and E. Mani, *Soft Matter*, 2023, **19**, 199–207.
- 6 M. Reifarh, M. Bekir, A. M. Bapolisi, E. Titov, F. Nußhardt, J. Nowaczyk, D. Grigoriev, A. Sharma, P. Saalfrank, S. Santer, M. Hartlieb and A. Böker, *Angew. Chem., Int. Ed.*, 2022, **61**, e202114687 (*Angew. Chem.*, 2022, **134**, e202114687).
- 7 C. Zhai, U. Azhar, W. Yue, Y. Dou, L. Zhang, X. Yang, Y. Zhang, P. Xu, C. Zong and S. Zhang, *Langmuir*, 2020, **36**, 15423–15429.
- 8 E. Chevallier, A. Saint-Jalmes, I. Cantat, F. Lequeux and C. Monteux, *Soft Matter*, 2013, **9**, 7054–7060.
- 9 M. Schnurbus, M. Hardt, P. Steinforth, J. Carrascosa-Tejedor, S. Winnall, P. Gutfreund, M. Schönhoff, R. A. Campbell and B. Braunschweig, *ACS Appl. Mater. Interfaces*, 2022, **14**, 4656–4667.
- 10 S. H. Kwon, M. Xu, J. Kim, E. J. Kim, Y. J. Lee, S. G. Jang, H. Yun and B. J. Kim, *Chem. Mater.*, 2021, **33**, 9769–9779.
- 11 J. Kim, H. Yun, Y. J. Lee, J. Lee, S.-H. Kim, K. H. Ku and B. J. Kim, *J. Am. Chem. Soc.*, 2021, **143**, 13333–13341.
- 12 R. F. Tabor, M. J. Pottage, C. J. Garvey and B. L. Wilkinson, *Chem. Commun.*, 2015, **51**, 5509–5512.
- 13 S. Chen, R. Costil, F. K.-C. Leung and B. L. Feringa, *Angew. Chem., Int. Ed.*, 2021, **60**, 11604–11627.
- 14 H. Oh, A. M. Ketner, R. Heymann, E. Kesselman, D. Danino, D. E. Falvey and S. R. Raghavan, *Soft Matter*, 2013, **9**, 5025–5033.
- 15 H. Sakai, Y. Orihara, H. Kodashima, A. Matsumura, T. Ohkubo, K. Tsuchiya and M. Abe, *J. Am. Chem. Soc.*, 2005, **127**, 13454–13455.
- 16 S. Peng, Q. Guo, T. C. Hughes and P. G. Hartley, *Langmuir*, 2014, **30**, 866–872.
- 17 C. S. G. Butler, L. W. Giles, A. V. Sokolova, L. de Campo, R. F. Tabor and K. L. Tuck, *Langmuir*, 2022, **38**, 7522–7534.
- 18 N. Basílio and L. Garcia-Río, *Curr. Opin. Colloid Interface Sci.*, 2017, **32**, 29–38.
- 19 G. Tyagi, J. L. Greenfield, B. E. Jones, W. N. Sharratt, K. Khan, D. Seddon, L. A. Malone, N. Cowieson, R. C. Evans, M. J. Fuchter and J. T. Cabral, *JACS Au*, 2022, **2**, 2670–2677.
- 20 C. E. Weston, R. D. Richardson, P. R. Haycock, A. J. P. White and M. J. Fuchter, *J. Am. Chem. Soc.*, 2014, **136**, 11878–11881.
- 21 M. Bekir, J. Gurke and M. Reifarh, *ChemSystemsChem*, 2024, **6**, e202400026.
- 22 D. A. Holden, H. Ringsdorf, V. Deblauwe and G. Smets, *J. Phys. Chem.*, 1984, **88**, 716–720.
- 23 S. Seshadri, S. J. Bailey, L. Zhao, J. Fisher, M. Sroda, M. Chiu, F. Stricker, M. T. Valentine, J. Read de Alaniz and M. E. Helgeson, *Langmuir*, 2021, **37**, 9939–9951.
- 24 H. Sakai, H. Ebana, K. Sakai, K. Tsuchiya, T. Ohkubo and M. Abe, *J. Colloid Interface Sci.*, 2007, **316**, 1027–1030.
- 25 K. Sakai, Y. Imaizumi, T. Oguchi, H. Sakai and M. Abe, *Langmuir*, 2010, **26**, 9283–9288.
- 26 K. Sakai, R. Yamazaki, Y. Imaizumi, T. Endo, H. Sakai and M. Abe, *Colloids Surf., A*, 2012, **410**, 119–124.
- 27 R. Klajn, *Chem. Soc. Rev.*, 2014, **43**, 148–184.
- 28 O. Glatter, *Scattering methods and their application in colloid and interface science*, Elsevier, 2018.
- 29 J. N. Israelachvili, in *Intermolecular and Surface Forces*, ed. J. N. Israelachvili, Academic Press, San Diego, 2011, pp. 503–534.
- 30 C. Blayo, J. E. Houston, S. M. King and R. C. Evans, *Langmuir*, 2018, **34**, 10123–10134.

